

ReasonNavi: Human-Inspired Global Map Reasoning for Zero-Shot Embodied Navigation

Yuzhuo Ao^{*1} Anbang Wang^{*1} Yu-Wing Tai² Chi-Keung Tang¹

¹The Hong Kong University of Science and Technology ²Dartmouth College

Abstract

*Embodied agents often struggle with efficient navigation because they rely primarily on partial egocentric observations, which restrict global foresight and lead to inefficient exploration. In contrast, humans plan using maps: we reason globally first, then act locally. We introduce **ReasonNavi**, a human-inspired framework that operationalizes this reason-then-act paradigm by coupling Multimodal Large Language Models (MLLMs) with deterministic planners. ReasonNavi converts a top-down map into a discrete reasoning space by room segmentation and candidate target nodes sampling. An MLLM is then queried in a multi-stage process to identify the candidate most consistent with the instruction (object, image, or text goal), effectively leveraging the model’s semantic reasoning ability while sidestepping its weakness in continuous coordinate prediction. The selected waypoint is grounded into executable trajectories using a deterministic action planner over an online-built occupancy map, while pretrained object detectors and segmenters ensure robust recognition at the goal. This yields a **unified zero-shot navigation framework** that requires no MLLM fine-tuning, circumvents the brittleness of RL-based policies and scales naturally with foundation model improvements. Across three navigation tasks, ReasonNavi consistently outperforms prior methods that demand extensive training or heavy scene modeling, offering a scalable, interpretable, and globally grounded solution to embodied navigation. Project page: <https://reasonnavi.github.io/>*

1. Introduction

Embodied AI agents often face challenges in efficient navigation due to reliance on partial, egocentric observations, which limit global foresight leading to suboptimal, meandering trajectories. While existing methods incorporate global map information, these approaches are typically task-specific, require extensive training, or struggle to gen-

eralize across diverse goal types [13, 22]. In contrast, humans navigate by reasoning globally over maps before acting locally, enabling strategic planning even with coarse 2D floor plans and minimal real-time exploration. This contrast motivates a central question: *Can we endow embodied agents with human-inspired global map reasoning to enable zero-shot, goal-directed navigation across diverse tasks?*

Multimodal Large Language Models (MLLMs) appear promising for this challenge. When presented with a floor plan and an instruction such as “Bring the mug from the kitchen to the bedroom,” current MLLMs can generate plausible high-level plans in a zero-shot manner. However, when tasked with embodied navigation, these models struggle. The reason lies in a fundamental mismatch: MLLMs are optimized for semantic reasoning, not for producing precise spatial coordinates or continuous control signals. They are excellent global reasoners but poor spatial controllers.

Our key insight is to embrace this mismatch by decomposing navigation into two complementary components. Instead of asking an MLLM to directly output coordinates, we transform navigation into a discrete reasoning problem. A set of well-distributed candidates is first generated using Poisson Disk Sampling over a top-down map. The MLLM then reasons in a multi-stage querying process to select the candidate that best aligns with the instruction, effectively leveraging its semantic reasoning capabilities while sidestepping its weakness in continuous spatial prediction. This global reasoning process is further strengthened by incorporating a model ensemble strategy to enhance robustness and accuracy. Once a target coordinate is selected, we ground this global plan into an executable trajectory using deterministic algorithms. Specifically, a hybrid A* + VFH* planner, operating on an online, wall-aware occupancy map, ensures reliable local path execution and collision avoidance. Robust recognition at the goal is achieved with pretrained detection and segmentation models.

This design yields several distinct advantages over prior work. By explicitly separating high-level reasoning from low-level control, ReasonNavi implements a human-inspired *reason-then-act* paradigm that produces in-

^{*}Equal contribution

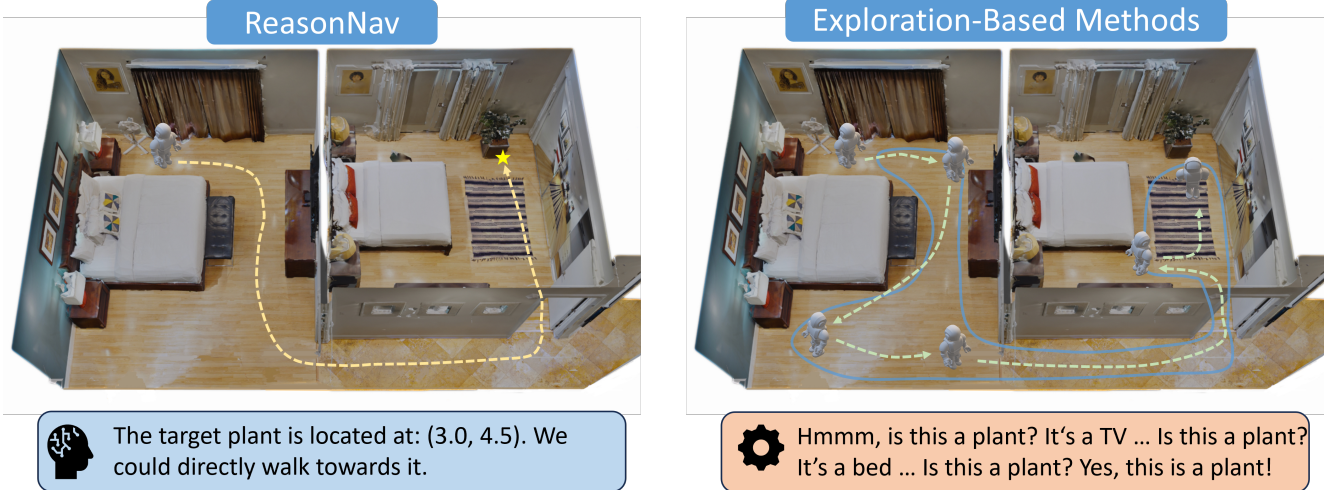


Figure 1. Main difference between our ReasonNavi and previous exploration-based methods: in ReasonNavi, after reasoning and obtaining the location of the desired target, the controlled agent will directly walk towards the object, whereas exploration-based methods heavily rely on extensive local semantic recognition or matching.

terpretable plans and avoids the inefficiency of reactive, exploration-heavy strategies, as shown in Figure 1. Because the framework relies purely on zero-shot reasoning without task-specific fine-tuning, ReasonNavi unifies object-goal, image-goal, and text-goal navigation in a single framework, in contrast to fragmented approaches requiring separate models or training pipelines. Deterministic planners provide robustness and generalization, eliminating the instability, sample inefficiency, and sim-to-real challenges commonly faced by reinforcement learning methods. Finally, ReasonNavi naturally benefits from ongoing improvements in foundation models: as MLLMs become stronger, their global reasoning quality directly enhances navigation performance, making the framework inherently scalable and future-proof.

In summary, our contributions are as follows:

- We propose **ReasonNavi**, a novel framework that integrates MLLM-based global reasoning with deterministic local planning, enabling a human-inspired *reason-then-act* paradigm for embodied navigation.
- ReasonNavi provides a unified, zero-shot solution to diverse navigation tasks, including object-goal, image-goal, and text-goal navigation, without requiring task-specific fine-tuning or reinforcement learning.
- By reframing navigation as discrete global reasoning followed by robust grounding with A* + VFH*, ReasonNavi achieves superior efficiency, reliability, and interpretability compared to prior approaches that rely on reactive exploration or complex scene modeling.

2. Related Work

Goal-Oriented Navigation. Recent advances in embodied navigation can be broadly categorized into end-to-end

learning-based methods and construction-based planning approaches. End-to-end methods, often based on reinforcement learning (RL), encode visual observations and directly predict low-level actions [2, 15–17, 19, 24–26]. While effective for short-term action prediction, these approaches often struggle to capture long-horizon dependencies and efficiently memorize fine-grained context, limiting their ability to plan globally.

Construction-based planning methods address this limitation by building structured representations of the environment, such as top-down semantic maps [10–12, 32], value maps [14, 29], or 3D scene graphs [27, 28, 36]. These methods update the map dynamically using online observations, enabling more informed path planning. However, because the map is constructed incrementally from local observations, global planning remains constrained, and agents may take sub-optimal paths or incur unnecessary exploration. Offline methods ([23]; [8]) build dense, open-vocabulary 3D scene graphs prior to navigation, offering richer semantic priors but at the cost of significant computational overhead and long reconstruction times, which limits real-time applicability. Overall, while construction-based approaches improve over purely reactive RL agents, they either depend on dense pre-built representations or remain limited by incremental local observations, leaving room for more flexible and scalable global reasoning.

Large Pretrained Models in Embodied Navigation.

The emergence of multimodal large language models (MLLMs) has introduced a new paradigm for navigation, leveraging their common-sense reasoning and generalization capabilities [1, 4–6, 30]. Following the Vision-Language-Action (VLA) paradigm [1], methods such as Navid [31], NaviLLM [33], and OctoNav [7] fine-tune MLLMs to directly map visual observations and instruc-

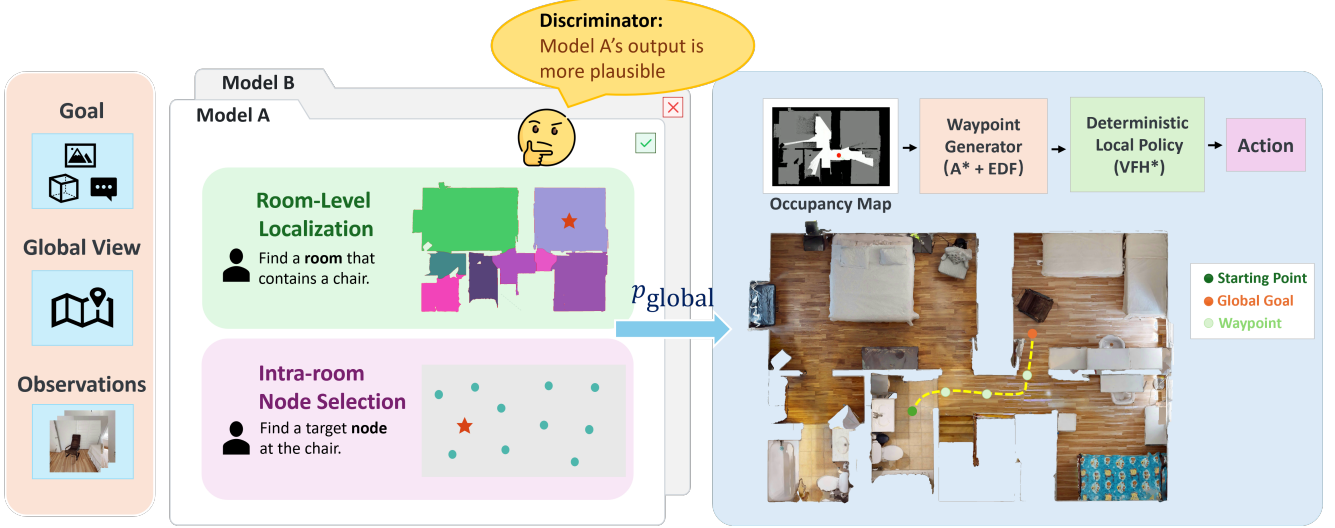


Figure 2. **The ReasonNavi Framework** in two stages: 1) Global Reasoning, where a Multimodal Large Language Model (MLLM) reasons about a top-down map and the goal instruction through a multi-stage discrete selection process to determine a precise global target waypoint (p_{global}). This MLLM reasoning stage can be further enhanced by a model ensemble for increased robustness; 2) Local Navigation, where a deterministic planner safely guides the agent to the selected global waypoint using an online occupancy map.

tions to low-level actions. Zero-shot approaches like NavGPT [34] and ESC [35] instead encode the agent’s observation and action history as textual prompts to guide decision-making. Despite their reasoning power, invoking MLLMs at every timestep incurs high computational cost and latency, challenging real-time deployment.

Limitations and Opportunities. Taken together, prior work highlights a key trade-off: end-to-end RL methods offer reactive control but limited global foresight; construction-based methods improve planning but depend on incremental or dense scene representations; and MLLM-based methods excel at reasoning but are computationally expensive and often disconnected from robust low-level control. Our work, ReasonNavi, addresses these gaps by combining the strengths of each paradigm: we leverage MLLM reasoning for global, zero-shot goal selection over a top-down map, while using deterministic planning for reliable local navigation. As shown in Figure 1, different from all the prior exploration-based methods, this integration enables interpretable, efficient, and scalable navigation without relying on dense scene reconstructions or fine-tuning the LLM, directly addressing the limitations of previous approaches.

3. Method

In this section, we present the architecture of our framework, as illustrated in Figure 2. We first define our versatile navigation tasks, then describe our hierarchical global reasoning module that identifies a target coordinate on a 2D map. We subsequently explain the local navigation policy for reaching this target and conclude with a model ensemble strategy for improved robustness.

3.1. Versatile Goal Navigation

Task Definition. We formulate our goal-oriented navigation task as follows: An embodied agent is deployed in an indoor environment E . The agent’s objective is to navigate to a goal g , which in turn defines a target object instance O or multiple possible instances within object category c in the environment. The goal g can be specified in one of three ways, defining three distinct sub-tasks: Object-goal Navigation, ON [3], where g is an object category, Instance-Image-goal Navigation, IIN [9], where g is an image containing object that can be found in the scene and Text-goal Navigation, TN [19], where g is a description about a certain object.

The agent is initialized at an arbitrary starting pose $p_0 \in E$. At each timestep t , the agent receives an egocentric RGB-D observation o_t . It also has access to a global 2D map M and its own pose p_t localized within this map. Based on these inputs, the agent must select an action a_t from a discrete action space $\mathcal{A} = \{\text{move_forward}, \text{turn_left}, \text{turn_right}, \text{stop}\}$. The task is successfully done if the agent stops within d meters of O in less than T time steps.

Task Specification. Unlike traditional goal-oriented navigation, which requires extensive exploration in the unseen environments, we consider zero-shot object navigation with global information: the task necessitates reasoning on the global view, the goal g can be freely specified with text (category or description) or image and the navigation system works in a training-free manner.

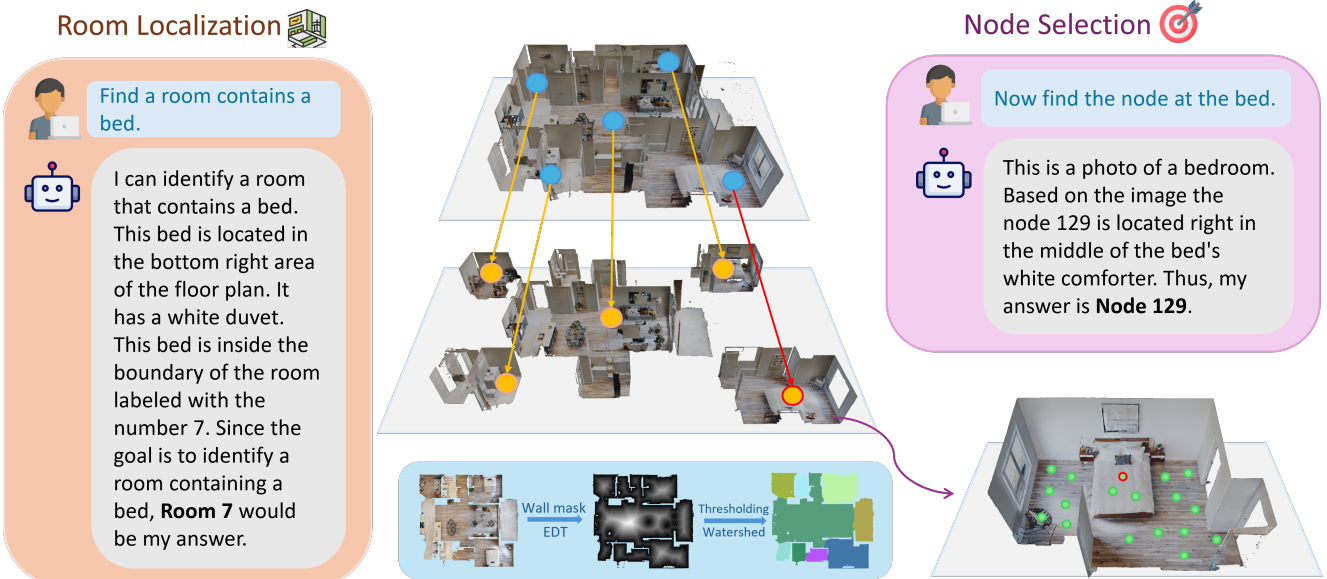


Figure 3. For global reasoning, instead of querying the MLLM for a direct coordinate, we devise a hierarchical, two-stage framework, which effectively leverages MLLM’s vision priors.

3.2. Global Reasoning

The global reasoning module aims to translate the goal description into a specific, long-term navigational goal on the 2D map, denoted as a coordinate p_{global} . To achieve this, we leverage the inherent commonsense and spatial reasoning capabilities of a Multi-modal Large Language Model (MLLM). Instead of directly regressing coordinates, which is often imprecise for MLLMs, we propose a hierarchical, coarse-to-fine framework. As illustrated in Figure 3, this two-stage approach first localizes the target to a specific room and then pinpoints a location within it, efficiently pruning the search space and simplifying the reasoning task.

Room-Level Localization. The first stage narrows the search down to a single room or a distinct region. We begin by processing the global 2D map to create a structured representation suitable for the MLLM. First, a binary wall mask M_0 is extracted using thresholding. For room segmentation, we apply Euclidean Distance Transform on M_0 and derive a number of isolated region seeds by thresholding Euclidean Distance Field (EDF). Then we apply the Watershed algorithm on these region seeds to obtain 2D region masks. This process partitions the entire floor plan into a set of unlabeled, segmented regions. To avoid that the rooms are incorrectly over-segmented, we then merge the tiny regions and derive the final region set $R = \{r_1, r_2, \dots, r_k\}$:

$$R = \text{Merge}(\text{Watershed}(\text{EDT}(M_0, d_{th}), M_0))$$

where d_{th} is the distance threshold to achieve the region seeds on the EDF. Please see B for details.

We then generate an annotated map $M(R)$ labeling each region. The MLLM is prompted with this map and a query

$P_1(g)$ to select the most probable room r^* . For ON and TN, the prompt is purely text. For IIN, the prompt also contains a goal image of O . The MLLM analyzes the spatial layout to identify the target room:

$$r^* = \text{MLLM}(M(R), P_1(g)) = \arg \max_{r_j \in R} P(g \text{ in } r_j \mid M)$$

where $P(g \text{ in } r_j \mid M)$ represents the likelihood of finding the target object g in room r_j , given the map M . The output of this stage is the selected room r^* .

Intra-Room Node Selection. To avoid the difficulty of regressing continuous coordinates, we discretize the entire navigable area of the global map into a set of candidate points. Leveraging the wall mask M_0 obtained from map preprocessing, we employ Poisson Disk Sampling (PDS) with a sampling radius of d_s on all navigable areas (i.e., regions not covered by M_0). PDS ensures that the sampled nodes are uniformly distributed and maintain a minimum distance from each other, providing good coverage and density across the entire map. This process generates a global set of candidate nodes, N_{global} .

Upon selecting a target room r^* , we then filter N_{global} to obtain a subset of candidate nodes $N = \{n_1, n_2, \dots, n_m\}$ that are located strictly within r^* . We then generate an annotated map, showing the cropped view of room r^* with these nodes marked with unique numbers. The MLLM is then prompted with the original cropped map M_{r^*} of room r^* , the node-annotated room map $M_{r^*}(N)$, along with the designed prompt $P_2(g)$ to the goal g , selecting the most

plausible node $n^* \in N$:

$$\begin{aligned} n^* &= \text{MLLM}(M_{r^*}(N), M_{r^*}, P_2(g)) \\ &= \arg \max_{n_j \in N} P(g \text{ at } n_j \mid M_{r^*}) \end{aligned}$$

where M_{r^*} is the map of the selected room. The 2D coordinates of this chosen node n^* become the final global goal, p_{global} , which is then passed to the local navigation method.

3.3. Local Navigation and Target Verification

Local Navigation. The local navigation module guides the agent safely and efficiently to the global target p_{global} . Unlike conventional navigation, p_{global} often lies in unexplored regions, meaning a complete, direct path may not exist in the agent’s current map. Our approach employs a hierarchical control strategy to dynamically plan collision-free and optimal paths.

Central to the navigator is an online occupancy map, acting as the agent’s long-term memory. This map categorizes areas into explored, unexplored, and occupied. Initially, occupied areas are defined by the wall mask M_0 , with continuous updates from RGB-D observations during navigation.

To navigate towards p_{global} , A* search is executed every T timesteps on the latest occupancy map to find an optimal path. A short-term waypoint w_t , d_0 meters ahead along this path, then serves as the immediate goal for the low-level controller. EDF, derived from EDT, acts as an additional costmap during A* search to ensure waypoints avoid walls and obstacles.

For reactive, collision-free movement towards w_t , the Vector Field Histogram* (VFH*) algorithm [20] computes steering commands by analyzing local obstacles in the occupancy map. A safety check ensures robustness: if online map updates reveal w_t or p_{global} is within an occupied area, the point is immediately relocated to the nearest valid, non-occupied location, preventing the agent from getting stuck. The agent iteratively follows these waypoints. Local navigation terminates and transitions to the target verification phase when the agent reaches a predefined proximity to p_{global} .

Target Verification. Upon reaching this first proximity threshold, the agent transitions into a verification mode to confirm the presence of the target object O . At every time step, the agent attempts to detect the target object within its current field of view using an object detector.

If no confident detection for the target category c is made in this initial view, the agent performs a final short approach to a second, closer proximity threshold, using VFH* with the original p_{global} as its waypoint. If still no detection at this second threshold, the agent then performs a 360-degree in-place scan. At each rotational step, the egocentric RGB image is processed by the object detector.

If a confident detection for the target category c is made at any stage of the verification process, we proceed to precise 3D localization. The 2D bounding box is fed to MobileSAM for precise segmentation mask generation. This mask isolates corresponding depth image points, which are then back-projected using camera intrinsics to form a 3D point cloud of the target. Its centroid in the occupancy map is computed to determine the object’s exact position. The agent then navigates to this precise position using VFH* with the detected object’s centroid as its waypoint, and executes a ‘stop’ action, completing the task. If the agent completes the 360-degree scan without any confident detections, the ‘stop’ action is called as well.

3.4. Model Ensemble

To further enhance performance in global reasoning, we design an additional plug-and-play component that integrates the strengths of different models. For our global reasoning task “locating objects from a top-down map”, it typically lacks large-scale datasets for MLLM training. We recognize that different MLLMs exhibit varying capabilities and limitations across different scenarios. This implies that simply switching to another model might not always significantly enhance performance. Therefore, we propose a model ensemble approach, introducing an additional discriminator to select the more plausible p_{global} from those provided by Model A and Model B. This aims to strengthen the performance of our global reasoning component.

Specifically, we employ two independent Global Reasoning (GR) units, denoted as GR_A and GR_B . These two units are based on different MLLMs A and B. Each reasoning unit independently receives the global 2D map M and the goal g , and performs room-level localization and intra-room node selection to generate a candidate global target point:

$$\begin{aligned} p_{\text{global}}^A &= \text{GR}_A(M, g) \\ p_{\text{global}}^B &= \text{GR}_B(M, g) \end{aligned}$$

To enable the discriminator to compare these two candidate points, we visualize them on the map. We generate two cropped annotated maps: M_A and M_B , where p_{global}^A and p_{global}^B are marked on two cropped map M_a and M_b from M respectively.

Subsequently, these two annotated maps, along with the original goal g , are fed into an additional discriminator MLLM. The task of this discriminator MLLM is to evaluate which candidate point better aligns with the semantics of goal g , based on its understanding of the map layout and the goal description. The discriminator is guided by a carefully designed prompt P_{dis} that encourages the MLLM to perform “self-verification,” comparing the plausibility of the two proposals,

$$p_{\text{global}}^{\text{final}} = \text{Discriminator}(M_A, M_B, P_{\text{dis}}(g))$$

The discriminator MLLM then outputs the global target point $p_{\text{global}}^{\text{final}}$ that it deems most plausible. This finally selected $p_{\text{global}}^{\text{final}}$ is then passed to the local navigation module, serving as the ultimate target for the agent’s navigation. This ensemble approach leverages the complementary strengths of multiple MLLMs and enhances the robustness and accuracy of global reasoning through the discriminator’s verification mechanism.

4. Experiments

We validate our framework through extensive experiments, comparing it with state-of-the-art methods across multiple benchmarks. Ablation studies confirm the effectiveness of our core components, and qualitative results demonstrate its generalization to complex scenarios like multi-floor and multi-agent navigation.

4.1. Experiment Setup

Benchmarks. We evaluate our ReasonNavi framework on object-goal, image-goal and text-goal navigation. For object-goal, we conduct experiments on the widely used Habitat-Matterport 3D (HM3D) 2022 challenge benchmark. For image-goal and text-goal navigation, we compare with other methods on HM3D 2023 ImageNav challenge and TextNav following Sun et al. [19].

Implementation Details. Our evaluation was conducted in Habitat-sim. We set the maximum time steps $T = 500$, with a linear step size of 0.25m and an angular rotation of 30 degrees per action. We also set the success threshold $d = 1\text{m}$. In our PDS sampling process, we use a sampling radius of 0.5m. We used Seed-1.6-thinking and Gemini-2.5 pro as global reasoning model, while utilizing GPT-5 as discriminator. Detailed prompts we are using are provided in Appendix.

Evaluation Metrics. We use two standard metrics: Success Rate (SR), the percentage of successful episodes, and Success weighted by Path Length (SPL), which measures path efficiency. If an episode is successful, $\text{SPL} = \frac{\text{Optimal Path Length}}{\text{Path Length}}$, otherwise $\text{SPL} = 0$.

4.2. Comparison with State-of-the-art

We compare ReasonNavi with the state-of-the-art goal-oriented navigation methods of different settings across three tasks in Table 1.

Object-goal Navigation. ReasonNavi achieves the highest SPL among all methods, including trained ones, underscoring its superior path efficiency. Our significantly higher SR and SPL highlights our ability to find more direct paths to the goal.

Image-goal Navigation. ReasonNavi adopts a unified framework for all navigation tasks, which means it relies on object detectors for final target verification in ImgNav,

rather than specialized similarity matching techniques. This design choice, while ensuring broad applicability, leads to an SR (47.8%) that is slightly lower than some highly specialized methods. However, ReasonNavi still achieves the highest SPL (30.4%) in this category. This high SPL stems directly from our global reasoning, which pinpoints a precise waypoint and eliminates the need for the extensive local exploration and matching required by other methods.

Text-goal Navigation. The inherent strength of ReasonNavi’s MLLM-powered global reasoning is particularly evident in TextNav. Here, our framework demonstrates clear dominance, achieving the best performance across all metrics with an SR of 38.8% and an SPL of 24.3%. This significantly surpasses other methods like GOAT [2] and UniGoal [28], highlighting ReasonNavi’s superior ability to interpret complex textual instructions and translate them into precise navigation goals in a zero-shot manner.

In summary, ReasonNavi’s strength lies in its human-like global reasoning, which translates diverse goals into precise map coordinates. This training-free, unified approach consistently yields high SPL by enabling direct, efficient paths to the target, setting a new benchmark for zero-shot navigation, especially in text-goal tasks where its semantic understanding excels.

4.3. Ablation Study

In our ablation study, we validate the effectiveness of our proposed multi-stage selection module and conduct experiments to compare the performance of different reasoning LLMs.

Ablation on our multi-stage selection. Our ablation study, presented in Table 2, clearly demonstrates the efficacy of our multi-stage selection strategy. Directly predicting continuous 3D coordinates yielded extremely low performance (SR 12.3%, SPL 6.13%), indicating the MLLM’s difficulty in regressing precise spatial coordinates and underscoring the necessity of selecting discrete, navigable nodes. While single-stage selection, which involves the MLLM choosing from the entire global topological graph, showed improved results (SR 44.5%, SPL 23.5%). However, it still shows asking the MLLM to select the optimal node from a vast global graph in a single step remains a challenging task. In contrast, our proposed multi-stage selection method achieved the best performance (SR 55.1%, SPL 29.6%), significantly outperforming single-stage selection (SR by 10.6%, SPL by 6.1%). This ablation study thus clearly confirms the superiority of ReasonNavi’s multi-stage node selection strategy, demonstrating that its hierarchical decision-making, which breaks down the complex target selection task into more manageable steps, enables the MLLM to reason and select targets with greater precision and robustness.

Ablation on different reasoning MLLMs. To eval-

Table 1. Results of Obj-goal, Image-goal and Text-goal navigation on HM3D challenge benchmarks. We compare the SR and SPL of state-of-the-art methods in different settings.

Method	Training -Free	ObjNav		ImgNav		TextNav	
		SR	SPL	SR	SPL	SR	SPL
OVRL-v2 [24]	×	64.7	28.1	—	—	—	—
OVRL-v2-IIN [24]	×	—	—	24.8	11.8	—	—
IEVE [12]	×	—	—	70.2	25.2	—	—
PSL [19]	×	42.4	19.2	23.0	11.4	16.5	7.5
GOAT [2]	×	50.6	24.1	37.4	16.1	17.0	8.8
ESC [35]	✓	39.2	22.3	—	—	—	—
OpenFMNav [11]	✓	54.9	24.4	—	—	—	—
Mod-IIN [10]	✓	—	—	56.1	23.3	—	—
SG-Nav [27]	✓	54.0	24.9	—	—	—	—
VLFM [29]	✓	52.5	30.4	—	—	—	—
Trihelper [32]	✓	56.5	25.3	—	—	—	—
UniGoal [28]	✓	54.5	25.1	60.2	23.7	20.2	11.4
ReasonNavi (ours)	✓	57.9	31.4	47.8	30.4	38.8	24.3

Table 2. Ablation study on the selection module. We compare our proposed multi-stage selection against direct coordinate prediction, and a single-stage baseline on the HM3D ObjNav challenge dataset. We are using Seed-1.6-Thinking as reasoning model in this experiment.

Selection Method	SR	SPL
Direct coordinate prediction	12.3	6.13
Single-stage selection	44.5	23.1
Multi-stage selection	55.1	29.6

uate the impact of the reasoning engine on our framework, we benchmarked several MLLMs, including the open-source Qwen2.5-7B-VL, and the advanced proprietary models Seed-1.6-Thinking and Gemini-2.5-Pro. The results, detailed in Table 3, show a clear correlation between the model’s reasoning capabilities and navigation performance. The advanced reasoning models, Seed-1.6-Thinking and Gemini-2.5-Pro, achieves significantly better performance compared with the smaller model across all the tasks, highlighting the importance of advanced reasoning for complex spatial understanding for our framework. Gemini-2.5-pro and Seed-1.6-Thinking generally derive similar results in object-goal navigation and image-goal navigation. However, possibly due to stronger capability in text understanding and reasoning, Gemini-2.5-pro outperforms Seed-1.6-Thinking with a large margin on TextNav. To maximize performance, we implement the model ensemble strategy in our method. This approach yielded the best results across all tasks. This demonstrates that ensembling leverages the diverse strengths of each model, mitigating individual weaknesses and leading to more robust and accurate navigation decisions.

This analysis confirms that advanced MLLMs are critical for performance. Our model ensemble strategy, by leveraging the complementary strengths of different models, consistently achieves the best results and pushes our framework

to state-of-the-art performance.

4.4. Qualitative Analysis

4.4.1. Navigation in Multi-Floor scenarios

Despite the inherent challenges of precisely controlling an agent to traverse between different floors via stairs in a zero-shot scenario, our proposed method exhibits powerful inter-floor reasoning abilities. As indicated in Figure 4a, when a target object is localized on a distinct floor, we utilize Chain-of-Thought (CoT) to decompose the complex multi-floor path into a series of single-floor navigation tasks, specifically, moving from the current position to the stairs, and then from the stairs to the target. This represents a crucial step beyond traditional single-floor navigation paradigms, enabling agents to tackle more realistic and complex spatial reasoning tasks.

4.4.2. Navigation with Multiple Agents

In real-world scenarios, the presence of dynamic obstacles (e.g., moving objects) poses significant challenges to dense scene modeling approaches reliant on point cloud representations. This complexity leads to critical issues in multi-agent collaborative navigation, where concurrent operations within shared environments induce catastrophic interference in existing frameworks. Prior construction-based methods often rely on static or one-shot semantic information. The dynamic presence of additional agents can sub-



(a) Figure 4a: Our framework can tackle the multi- (b) Figure 4b: Our framework inherently allows (c) Figure 4c: A top-down map generated by VGGT floor task by decomposing it to single-floor tasks. multiple agents running in the same workspace. from 33 RGB images.

Table 3. Ablation study on different reasoning MLLMs. We report the performance of our framework when equipped with different large language models on the HM3D ObjNav, ImgNav, and TextNav datasets.

Reasoning MLLM	ObjNav		ImgNav		TextNav	
	SR	SPL	SR	SPL	SR	SPL
Qwen2.5-7B-VL	41.3	21.2	22.8	14.3	17.0	10.1
Seed-1.6-Thinking	55.1	29.6	40.2	25.2	30.1	19.0
Gemini-2.5-Pro	55.8	29.1	40.7	25.6	37.2	22.8
Model Ensemble	57.9	31.4	47.8	30.4	38.8	24.3

stantially interfere with their semantic understanding, leading to compromised navigation performance. As shown in Figure 4b, our approach, on the other hand, fundamentally differs by relying solely on depth data for local obstacle avoidance during navigation. This design choice inherently minimizes inter-agent conflicts, thereby demonstrating superior scalability and robustness in multi-agent environments.

5. Discussion

Our framework, ReasonNavi, operates under the assumption that a global, top-down 2D map of the environment is available prior to navigation. While this may appear to be a strong prerequisite, we argue that it is a practical and increasingly feasible assumption in many real-world robotics and embodied AI scenarios. The generation of such maps is no longer a significant bottleneck, as they can be sourced in multiple ways. For instance, our framework can directly utilize standard CAD floor plans, which are often readily available for structured environments. Even when such plans are absent, emerging technologies like Visual Geometry Grounded Transformer (VGGT) [21] can reconstruct a 3D model of an environment from unposed RGB images effectively, from which a top-down map can be extracted. As depicted in 4c, the map was reconstructed from only 33 RGB images in under 10 seconds. Crucially, our tests confirm that MLLMs can effectively parse the room structure

from such generated maps, validating their suitability for our global reasoning stage. In either case, this process can be performed offline as a one-time setup step, making it a reasonable pre-computation for deploying robotic agents.

6. Conclusion

In this paper, we introduce ReasonNavi, a novel, human-inspired framework for zero-shot embodied navigation. Our approach uniquely leverages the strengths of MLLMs for high-level hierarchical global reasoning, while relegating low-level control and execution to robust, deterministic planners. This “reason-then-act” paradigm sidesteps the challenges of using LLMs for precise, continuous control, a task for which they are not optimized. We demonstrate that only by focusing the MLLM’s role on a one-off global reasoning task with one global view image, we can achieve state-of-the-art (SOTA) performance in a computationally efficient manner. The framework’s zero-shot and computationally efficient nature eliminates the need for costly and time-consuming fine-tuning, RL training or real-time inference, making it a scalable and practical solution for a diverse range of embodied navigation tasks.

References

[1] Anthony Brohan, Noah Brown, Justice Carbajal, Yevgen Chebotar, Xi Chen, Krzysztof Choromanski, Tianli Ding, Danny Driess, Avinava Dubey, Chelsea Finn, Pete Florence, Chuyuan Fu, Montse Gonzalez Arenas, Keerthana Gopalakrishnan, Kehang Han, Karol Hausman, Alexander Herzog, Jasmine Hsu, Brian Ichter, Alex Irpan, Nikhil Joshi, Ryan Julian, Dmitry Kalashnikov, Yuheng Kuang, Isabel Leal, Lisa Lee, Tsang-Wei Edward Lee, Sergey Levine, Yao Lu, Henryk Michalewski, Igor Mordatch, Karl Pertsch, Kanishka Rao, Krista Reymann, Michael Ryoo, Grecia Salazar, Pannag Sanketi, Pierre Sermanet, Jaspair Singh, Anikait Singh, Radu Soricu, Huong Tran, Vincent Vanhoucke, Quan Vuong, Ayzaan Wahid, Stefan Welker, Paul Wohlhart, Jialin Wu, Fei Xia, Ted Xiao, Peng Xu, Sichun Xu, Tianhe Yu, and Brianna Zitkovich. Rt-2: Vision-language-action models transfer web knowledge to robotic control. *arXiv preprint arXiv:2307.15818*, 2023. 2

[2] Matthew Chang, Theophile Gervet, Mukul Khanna, Sriram Yenamandra, Dhruv Shah, So Yeon Min, Kavit Shah, Chris Paxton, Saurabh Gupta, Dhruv Batra, Roozbeh Mottaghi, Jitendra Malik, and Devendra Singh Chaplot. Goat: Go to any thing. *arXiv preprint arXiv:2311.06430*, 2023. 2, 6, 7

[3] Devendra Singh Chaplot, Dhiraj Gandhi, Abhinav Gupta, and Ruslan Salakhutdinov. Object goal navigation using goal-oriented semantic exploration. *arXiv preprint arXiv:2007.00643*, 2020. 3

[4] Jiaqi Chen, Bingqian Lin, Ran Xu, Zhenhua Chai, Xiaodan Liang, and Kwan-Yee K. Wong. Mapgpt: Map-guided prompting with adaptive path planning for vision-and-language navigation. *arXiv preprint arXiv:2401.07314*, 2024. 2

[5] Vishnu Sashank Dorbala, James F. Mullen, and Dinesh Manocha. Can an embodied agent find your “cat-shaped mug”? Ilm-based zero-shot object navigation. *IEEE Robotics and Automation Letters*, 9(5):4083–4090, 2024.

[6] Danny Driess, Fei Xia, Mehdi S. M. Sajjadi, Corey Lynch, Aakanksha Chowdhery, Brian Ichter, Ayzaan Wahid, Jonathan Tompson, Quan Vuong, Tianhe Yu, Wenlong Huang, Yevgen Chebotar, Pierre Sermanet, Daniel Duckworth, Sergey Levine, Vincent Vanhoucke, Karol Hausman, Marc Toussaint, Klaus Greff, Andy Zeng, Igor Mordatch, and Pete Florence. Palm-e: An embodied multimodal language model. *arXiv preprint arXiv:2303.03378*, 2023. 2

[7] Chen Gao, Liankai Jin, Xingyu Peng, Jiazhao Zhang, Yue Deng, Annan Li, He Wang, and Si Liu. Octonav: Towards generalist embodied navigation. *arXiv preprint arXiv:2506.09839*, 2025. 2

[8] Qiao Gu, Alihusein Kuwajerwala, Sacha Morin, Krishna Murthy Jatavallabhula, Bipasha Sen, Aditya Agarwal, Corban Rivera, William Paul, Kirsty Ellis, Rama Chellappa, Chuang Gan, Celso Miguel de Melo, Joshua B. Tenenbaum, Antonio Torralba, Florian Shkurti, and Liam Paull. Concept-graphs: Open-vocabulary 3d scene graphs for perception and planning. *arXiv preprint arXiv:2309.16650*, 2023. 2

[9] Jacob Krantz, Stefan Lee, Jitendra Malik, Dhruv Batra, and Devendra Singh Chaplot. Instance-specific image goal navigation: Training embodied agents to find object instances. *arXiv preprint arXiv:2211.15876*, 2022. 3

[10] Jacob Krantz, Theophile Gervet, Karmesh Yadav, Austin Wang, Chris Paxton, Roozbeh Mottaghi, Dhruv Batra, Jitendra Malik, Stefan Lee, and Devendra Singh Chaplot. Navigating to objects specified by images. In *ICCV*, pages 10916–10925, 2023. 2, 7

[11] Yuxuan Kuang, Hai Lin, and Meng Jiang. Openfmnav: Towards open-set zero-shot object navigation via vision-language foundation models. In *Findings of the Association for Computational Linguistics: NAACL 2024*, pages 338–351, 2024. 7

[12] Xiaohan Lei, Min Wang, Wengang Zhou, Li Li, and Houqiang Li. Instance-aware exploration-verification-exploitation for instance imagegoal navigation. In *IEEE/CVF Conference on Computer Vision and Pattern Recognition (CVPR)*, pages 16329–16339, 2024. 2, 7

[13] Jinzhou Lin, Han Gao, Xuxiang Feng, Rongtao Xu, Changwei Wang, Man Zhang, Li Guo, and Shibiao Xu. Advances in embodied navigation using large language models: A survey. *arXiv preprint arxiv:2311.00530*, 2025. 1

[14] Yuxing Long, Wenzhe Cai, Hongcheng Wang, Guanqi Zhan, and Hao Dong. Instructnav: Zero-shot system for generic instruction navigation in unexplored environment. *arXiv preprint arXiv:2406.04882*, 2024. 2

[15] Arjun Majumdar, Gunjan Aggarwal, Bhavika Devnani, Judy Hoffman, and Dhruv Batra. Zson: Zero-shot object-goal navigation using multimodal goal embeddings. *arXiv preprint arXiv:2206.12403*, 2023. 2

[16] Oleksandr Maksymets, Vincent Cartillier, Aaron Gokaslan, Erik Wijmans, Wojciech Galuba, Stefan Lee, and Dhruv Batra. Thda: Treasure hunt data augmentation for semantic navigation. In *IEEE/CVF International Conference on Computer Vision (ICCV)*, pages 15374–15383, 2021.

[17] Arsalan Mousavian, Alexander Toshev, Marek Fiser, Jana Kosecka, Ayzaan Wahid, and James Davidson. Visual representations for semantic target driven navigation. *arXiv preprint arXiv:1805.06066*, 2019. 2

[18] Dujun Nie, Xianda Guo, Yiqun Duan, Ruijun Zhang, and Long Chen. Wmnav: Integrating vision-language models into world models for object goal navigation. *arXiv preprint arXiv:2503.02247*, 2025. 16

[19] Xinyu Sun, Lizhao Liu, Hongyan Zhi, Ronghe Qiu, and Junwei Liang. Prioritized semantic learning for zero-shot instance navigation. In *European Conference on Computer Vision (ECCV)*, pages 161–178, 2025. 2, 3, 6, 7

[20] I. Ulrich and J. Borenstein. Vfh/sup */: local obstacle avoidance with look-ahead verification. In *Proceedings 2000 ICRA. Millennium Conference. IEEE International Conference on Robotics and Automation. Symposia Proceedings (Cat. No.00CH37065)*, pages 2505–2511 vol.3, 2000. 5

[21] Jianyuan Wang, Minghao Chen, Nikita Karaev, Andrea Vedaldi, Christian Rupprecht, and David Novotny. Vggt: Visual geometry grounded transformer. In *Proceedings of the IEEE/CVF Conference on Computer Vision and Pattern Recognition*, 2025. 8

[22] Congcong Wen, Yisiyuan Huang, Hao Huang, Yanjia Huang, Shuaihang Yuan, Yu Hao, Hui Lin, Yu-Shen Liu, and Yi

Fang. Zero-shot object navigation with vision-language models reasoning. *arXiv preprint arxiv:2410.18570*, 2024. 1

[23] Abdelrhman Werby, Chenguang Huang, Martin Büchner, Abhinav Valada, and Wolfram Burgard. Hierarchical Open-Vocabulary 3D Scene Graphs for Language-Grounded Robot Navigation. In *Proceedings of Robotics: Science and Systems*, 2024. 2

[24] Karmesh Yadav, Arjun Majumdar, Ram Ramrakhyा, Naoki Yokoyama, Alexei Baevski, Zsolt Kira, Oleksandr Maksymets, and Dhruv Batra. Ovrl-v2: A simple state-of-art baseline for imagenav and objectnav. *arXiv preprint arXiv:2303.07798*, 2023. 2, 7

[25] Wei Yang, Xiaolong Wang, Ali Farhadi, Abhinav Gupta, and Roozbeh Mottaghi. Visual semantic navigation using scene priors. *arXiv preprint arXiv:1810.06543*, 2018.

[26] Joel Ye, Dhruv Batra, Abhishek Das, and Erik Wijmans. Auxiliary tasks and exploration enable objectnav. *arXiv preprint arXiv:2104.04112*, 2021. 2

[27] Hang Yin, Xiuwei Xu, Zhenyu Wu, Jie Zhou, and Jiwen Lu. Sg-nav: Online 3d scene graph prompting for llm-based zero-shot object navigation. *arXiv preprint arXiv:2410.08189*, 2024. 2, 7

[28] Hang Yin, Xiuwei Xu, Lingqing Zhao, Ziwei Wang, Jie Zhou, and Jiwen Lu. Unigoal: Towards universal zero-shot goal-oriented navigation. *arXiv preprint arXiv:2503.10630*, 2025. 2, 6, 7

[29] Naoki Yokoyama, Sehoon Ha, Dhruv Batra, Jiuguang Wang, and Bernadette Bucher. Vlfm: Vision-language frontier maps for zero-shot semantic navigation. *arXiv preprint arXiv:2312.03275*, 2023. 2, 7

[30] Bangguo Yu, Hamidreza Kasaeei, and Ming Cao. L3mvn: Leveraging large language models for visual target navigation. In *IEEE/RSJ International Conference on Intelligent Robots and Systems (IROS)*, page 3554–3560, 2023. 2

[31] Jiazhao Zhang, Kunyu Wang, Rongtao Xu, Gengze Zhou, Yicong Hong, Xiaomeng Fang, Qi Wu, Zhizheng Zhang, and He Wang. Navid: Video-based vlm plans the next step for vision-and-language navigation. *arXiv preprint arXiv:2402.15852*, 2024. 2

[32] Lingfeng Zhang, Qiang Zhang, Hao Wang, Erjia Xiao, Zixuan Jiang, Honglei Chen, and Renjing Xu. Trihelper: Zero-shot object navigation with dynamic assistance. *arXiv preprint arXiv:2403.15223*, 2024. 2, 7

[33] Duo Zheng, Shijia Huang, Lin Zhao, Yiwu Zhong, and Liwei Wang. Towards learning a generalist model for embodied navigation. *arXiv preprint arXiv:2312.02010*, 2024. 2

[34] Gengze Zhou, Yicong Hong, and Qi Wu. Navgpt: Explicit reasoning in vision-and-language navigation with large language models. *arXiv preprint arXiv:2305.16986*, 2023. 3

[35] Kaiwen Zhou, Kaizhi Zheng, Connor Pryor, Yilin Shen, Hongxia Jin, Lise Getoor, and Xin Eric Wang. Esc: Exploration with soft commonsense constraints for zero-shot object navigation. In *International Conference on Machine Learning (ICML)*, 2023. 3, 7

[36] Ziyu Zhu, Xilin Wang, Yixuan Li, Zhuofan Zhang, Xiaojian Ma, Yixin Chen, Baoxiong Jia, Wei Liang, Qian Yu, Zhi-dong Deng, Siyuan Huang, and Qing Li. Move to understand a 3d scene: Bridging visual grounding and exploration for efficient and versatile embodied navigation. *arXiv preprint arXiv:2507.04047*, 2025. 2

Appendix

In this appendix, we present:

- Prompts used in ReasonNavi.
- Details of our method.
- Generalization to Diverse Map Modalities.
- Additional comparison with concurrent work.
- Limitations and future work.
- The use of large language models (LLMs)

A. Prompts used in ReasonNavi

We provide our detailed prompts used in ReasonNavi:

Room-Level Localization:

You are an AI assistant for a robot's navigation system. Your task is to identify a certain room.

CONTEXT: You will be provided with a top-down floor plan showing furniture and layout with room segmentation. (The floor plan is segmented to at least one room/region with numbered room annotations. The boundaries of different rooms are noted in white.)

GOAL: Identify the room number that contains the {goal_object}.

INSTRUCTIONS:

1. If you can find the object directly from map, describe the object's location using text.

2. **Analyze the Goal Object:** Determine the room number where the {goal_object} can be found. If you cannot find {goal_object} on the top-down view, then please consider the most-possible room that the {goal_object} may locate at. (e.g., a "bed" is in a bedroom)

3. **Verify the Room:** Scan the top-down view to make sure that the {goal_object} indeed locates in the chosen room. If {goal_object} cannot be found, make sure the chosen room is the most appropriate room to search.

Note that you should consider the precise semantics of {goal_object} during verification. (e.g., "sofa chair" is different from "sofa")

Note that you should choose the room that contains the {goal_object} instead of the room that is the closest to the {goal_object}!

Repeat the instruction until the verification (3.) is passed.

Provide your answer in the last line in the form of: "Room X" where X is your chosen number. (e.g. Room 1)

Goal Object: {goal_object}

where {goal_object} will be replaced by the goal g .

Intra-Room Node Selection:

CONTEXT: You are given two images:

1. **Map Image:** A top-down schematic of the room's layout.
2. **Node Image:** The same map with numbered navigation nodes.

GOAL: {goal_object}

INSTRUCTIONS:

1. **Analyze the Goal:** Consider the common placement of a {goal_object}. For example, a "TV" is opposite to sofa in the living room; a "book" is on a shelf or table. Note the **precise semantics** of {goal_object} and do not misunderstand the target. (e.g., **sofa chair** is different from **sofa**).

2. **Locate on Map:** Scan the Map Image to find the {goal_object} or the most logical place it would be (e.g., find the dining table if the goal is a "plate").

3. **Select Best Node:** Based on your location analysis, choose the single best node from the Node Image. The best node is determined by this priority:

* **Priority 1:** A node located directly on the object.

* **Priority 2:** If no node is on the object, the node closest to the object.

* **Priority 3:** If the object cannot be found on the topdown-view, the node that provides the best vantage point to search the inferred area.

4. **Verify The Node:** Make sure the selected node satisfy the above requirements.

Repeat the instructions until the verification (4.) is passed.

Goal Object: {goal_object} Provide your answer in the last line in the form of: "node X" where X is your chosen number. (e.g. node 100)

where {goal_object} will be replaced by the goal *g*.

Discriminator:

You are an expert navigation system evaluator. I need you to analyze a controversial episode where two different AI models disagreed on the success of an object navigation task.

Target Object: {goal_object}

Images Provided: You will see two separate images:

1. **First Image (Model 1):** Shows an area around Model 1's target selection with a **BLUE** circle marking the chosen target location.

2. **Second Image (Model 2):** Shows a area around Model 2's target selection with a **RED** circle marking the chosen target location.

Your Task: Please analyze these navigation scenarios and determine which model made the better decision. Consider:

1. **Target Identification:** Which model identified a more plausible target location for "{goal_object}"? Look at the environment around each colored circle, find the corresponding node that is closer to the {goal_object}.

2. **Accessibility:** If two nodes are both at a plausible position of the {goal_object}, which target location appears more accessible and reachable in a real navigation scenario? (i.e. more close to the navigable/walkable area and more close to the open space. (e.g. Two chairs. The one that is closer to the open area is more suitable than the one that is closer to the wall.))

Please respond with:

1. Your analysis of both models' target selections based on the environmental context
2. Which model you believe made the better decision (Model 1 or Model 2)
3. Key reasoning points for your decision

Output Format: Decision: [Model 1 or Model 2]

where {goal_object} will be replaced by the goal g .

B. Details of our method

B.1. Room Segmentation

Our room segmentation pipeline is designed to robustly partition a top-down floor plan into distinct room areas. The process leverages a combination of morphological operations, EDT, and the Watershed algorithm, followed by a post-processing step to merge small, erroneous room fragments.

The process begins with a binary wall mask, where non-walkable areas (walls) are distinguished from walkable spaces. A morphological closing operation is first applied to fill minor gaps and holes in the detected walls, ensuring that rooms are well-enclosed entities.

Subsequently, the EDT is computed on the walkable areas. The EDT assigns each pixel a value corresponding to its distance to the nearest wall. This transform is crucial as it allows us to identify the central, core regions of rooms—pixels with high distance values are far from any walls and are thus strong candidates for being region seeds.

The determination of these seeds is critical. For greater adaptability, we employ Otsu's method on the normalized and blurred distance map. This automatically finds an optimal threshold to separate the map into two classes: room cores (sure foreground) and areas closer to walls (ambiguous regions). This dynamic approach makes the segmentation robust to varying room sizes and layouts.

With the seeds (sure foreground) and walls (sure background) identified, the Watershed algorithm is applied. This algorithm treats the distance map as a topographical surface, “flooding” it from the seed locations until the “waters” from different seeds meet. These meeting lines form the boundaries that segment the space into initial room candidates.

Finally, a merging procedure is executed to handle over-segmentation, where small, insignificant regions might be incorrectly labeled as separate rooms. This iterative process identifies rooms smaller than a minimum area threshold and merges them into the most suitable adjacent larger room. The suitability is determined by a merge score that considers the length of

the shared boundary and the proximity of the room centroids, ensuring that merges are geometrically logical. The process is outlined in Algorithm 1.

Algorithm 1 Room Segmentation via EDT and Watershed

Require: Binary Wall Mask M_{binary}
Ensure: Labeled Marker Matrix M_{rooms}

```

 $M_{\text{closed}} \leftarrow \text{MorphologicalClose}(M_{\text{binary}})$ 
 $M_{\text{dist}} \leftarrow \text{EuclideanDistanceTransform}(M_{\text{closed}})$ 
 $M_{\text{norm}} \leftarrow \text{Normalize}(M_{\text{dist}}, \text{range} = [0, 255])$ 
 $M_{\text{blur}} \leftarrow \text{GaussianBlur}(M_{\text{norm}})$ 
 $T_{\text{Otsu}}, M_{\text{seeds}} \leftarrow \text{OtsuThreshold}(M_{\text{blur}})$ 
 $M_{\text{bg}} \leftarrow \text{Dilate}(M_{\text{closed}}, K)$ 
 $M_{\text{unknown}} \leftarrow M_{\text{bg}} - M_{\text{seeds}}$ 
 $M_{\text{markers}} \leftarrow \text{ConnectedComponents}(M_{\text{seeds}})$ 
 $M_{\text{markers}} \leftarrow M_{\text{markers}} + 1$ 
 $M_{\text{markers}}[M_{\text{unknown}} = \text{true}] \leftarrow 0$ 
 $M_{\text{rooms}} \leftarrow \text{Watershed}(M_{\text{closed}}, M_{\text{markers}})$ 
 $M_{\text{rooms}} \leftarrow \text{MergeSmallRooms}(M_{\text{rooms}})$ 
return  $M_{\text{rooms}}$ 

```

Algorithm 2 Node Generation via Multi-Region Poisson Disk Sampling

Require: Binary Walkable Mask M_{walkable} , Wall Padding Distance D_{padding} , PDS Radius R_{pds}
Ensure: Set of Navigation Nodes N_{all}

```
 $M_{\text{padded}} \leftarrow \text{Erode}(M_{\text{walkable}}, D_{\text{padding}})$ 
 $C_{\text{list}} \leftarrow \text{FindConnectedComponents}(M_{\text{padded}})$ 
 $N_{\text{all}} \leftarrow \emptyset$ 
for each component  $C$  in  $C_{\text{list}}$  do
     $N_{\text{active}} \leftarrow \emptyset$ 
     $N_{\text{component}} \leftarrow \emptyset$ 
     $G_{\text{grid}} \leftarrow \text{InitializeGrid}(C, R_{\text{pds}})$ 
     $p_{\text{initial}} \leftarrow \text{SelectRandomPointIn}(C)$ 
    Add  $p_{\text{initial}}$  to  $N_{\text{active}}$ ,  $N_{\text{component}}$ , and  $G_{\text{grid}}$ 
    while  $N_{\text{active}}$  is not empty do
         $p_{\text{current}} \leftarrow \text{SelectRandomPointFrom}(N_{\text{active}})$ 
         $p_{\text{found}} \leftarrow \text{false}$ 
        for  $i \leftarrow 1$  to  $k_{\text{attempts}}$  do
             $p_{\text{new}} \leftarrow \text{GeneratePointInAnnulus}(p_{\text{current}}, R_{\text{pds}}, 2R_{\text{pds}})$ 
            if  $\text{IsValid}(p_{\text{new}}, C, G_{\text{grid}}, R_{\text{pds}})$  then
                Add  $p_{\text{new}}$  to  $N_{\text{active}}$ ,  $N_{\text{component}}$ , and  $G_{\text{grid}}$ 
                 $p_{\text{found}} \leftarrow \text{true}$ 
                break
            end if
        end for
        if not  $p_{\text{found}}$  then
            Remove  $p_{\text{current}}$  from  $N_{\text{active}}$ 
        end if
    end while
     $N_{\text{all}} \leftarrow N_{\text{all}} \cup N_{\text{component}}$ 
end for
return  $N_{\text{all}}$ 
```

B.2. Nodes Generation

Our implementation begins with the binary walkable mask and applies a configurable wall padding. This is achieved through morphological erosion, which shrinks the walkable area by a specified distance. This crucial preprocessing step ensures that all generated navigation nodes maintain a safe distance from walls and obstacles, preventing the planner from creating paths that are too close to collisions.

Then we use an enhanced PDS algorithm to handle environments with multiple disconnected regions. First, a connected components analysis is performed on the padded walkable mask to identify all distinct, navigable areas. Then, the PDS algorithm is executed independently within each of these regions. This ensures that every separate walkable space is populated with navigation nodes, guaranteeing comprehensive coverage of the entire environment. The algorithm iteratively adds points by selecting a random point from an “active list,” generating new candidate points in an annulus around it, and validating that the new point respects the minimum distance constraint relative to all existing points. The process is outlined in Algorithm 2.

B.3. Local Navigation

The entire process is outlined in Algorithm 3.

Algorithm 3 Local Navigation and Target Verification

Require: Global goal p_{global} , Proximity thresholds $d_{\text{prox1}}, d_{\text{prox2}}$
Ensure: Navigation Stop

```
 $M_{\text{occ}} \leftarrow \text{InitializeMap}()$ 
while  $\text{distance}(\text{GetAgentPose}(), p_{\text{global}}) > d_{\text{prox1}}$  do
     $o_t \leftarrow \text{GetCurrentObservation}()$ 
     $M_{\text{occ}} \leftarrow \text{UpdateMap}(M_{\text{occ}}, o_t)$ 
     $P \leftarrow \text{A\_star\_Search}(M_{\text{occ}}, \text{GetAgentPose}(), p_{\text{global}})$ 
     $w_t \leftarrow \text{GetLocalWaypoint}(P)$ 
     $w_t \leftarrow \text{SafetyCheck}(w_t, M_{\text{occ}})$ 
     $\text{action} \leftarrow \text{VFH\_star\_Controller}(w_t, M_{\text{occ}})$ 
     $\text{Execute}(\text{action})$ 
end while
while  $\text{distance}(\text{GetAgentPose}(), p_{\text{global}}) > d_{\text{prox2}}$  do
     $\text{found}, p_{\text{obj}} \leftarrow \text{Scan360AndDetect}()$ 
    if  $\text{found}$  then
        break
    end if
     $\text{ApproachCloser}(p_{\text{global}})$ 
end while
if  $\text{not found}$  then
     $\text{found}, p_{\text{obj}} \leftarrow \text{Scan360AndDetect}()$ 
end if
if  $\text{found}$  then
     $p_{\text{final}} \leftarrow \text{LocalizeObject3D}(p_{\text{obj}})$ 
     $\text{NavigateToFinalPosition}(p_{\text{final}})$ 
end if
Navigation Stop
```

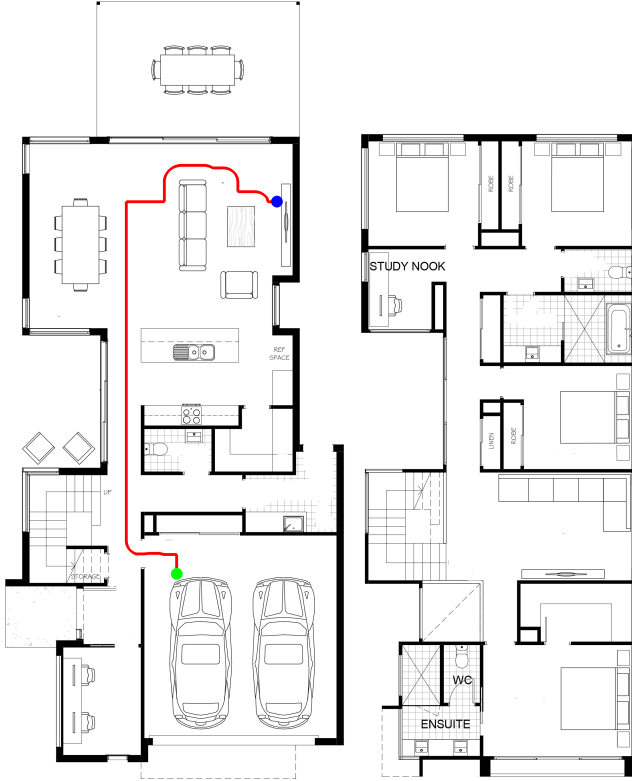
C. Generalization to Diverse Map Modalities

While the primary experiments in this work utilize top-down maps derived from detailed 3D reconstructions, the fundamental approach of ReasonNavi is not constrained to this specific map modality. The strength of leveraging an MLLM for global reasoning is its ability to interpret a wide variety of visual schematic representations. This allows our method to generalize seamlessly to other common and more accessible forms of spatial data, such as architectural CAD drawings or even noisy top-down maps generated from scans using standard mobile devices. As illustrated in Figure 5, the agent can successfully generate a navigation plan from a starting point (green dot) to a goal object’s inferred location (blue dot) on both a clean CAD floor plan and a reconstructed point-cloud map. This adaptability significantly broadens the potential real-world applicability of our framework, reducing the dependency on specialized 3D scanning hardware.

D. Additional comparison with concurrent work

During our research, we noted the concurrent development of WMNav [18], another framework that leverages Vision-Language Models (VLMs) for zero-shot object navigation. Both ReasonNavi and WMNav achieve state-of-the-art performance on the HM3D ObjectNav benchmark, demonstrating remarkably similar top-line metrics (ReasonNavi: 57.9% SR, 31.4% SPL; WMNav: 58.1% SR, 31.2% SPL). Despite these comparable results, the two methods are founded on fundamentally different philosophies regarding the role of the MLLM in navigation.

The core distinction lies in the source of visual understanding and the frequency of MLLM inference. ReasonNavi operates on a *global-view, one-off* reasoning paradigm. It leverages the MLLM’s powerful spatial and semantic understanding capabilities a single time at the beginning of an episode. By processing a complete top-down map, ReasonNavi formulates a comprehensive global plan, identifying a precise target coordinate (p_{global}) before the agent begins to move. This “reason-then-act” approach cleanly separates high-level strategic planning from low-level, deterministic execution, minimizing computational overhead and avoiding the risk of cumulative errors from repeated model inferences.



(a) Path planning on a CAD floor plan.



(b) Path planning on a top-down map from a mobile device reconstruction.

Figure 5. Demonstration of ReasonNavi’s generalization to diverse map modalities. The agent successfully plans a path from the start point (green) to the goal (blue) on both a clean CAD drawing and a reconstructed map.

In stark contrast, WMNav relies entirely on *local observations* and employs a *step-by-step* reasoning process. Its visual understanding is derived from panoramic images captured at the agent’s current position at each timestep. This approach necessitates a heavy, iterative reliance on the VLM throughout the exploration phase to interpret the immediate surroundings, predict the potential presence of the target in different directions, and update a “Curiosity Value Map”. While this allows the agent to react to newly observed information, it involves a substantial number of VLM calls, making the process computationally intensive and potentially susceptible to model hallucinations over long horizons.

In summary, while both frameworks successfully utilize the power of modern foundation models, ReasonNavi’s approach of using the MLLM for a single, decisive act of global reasoning based on a complete map proves to be a more efficient and robust strategy. Our significantly higher SPL, despite a marginal difference in SR, suggests that our global, one-off planning leads to more direct and efficient paths. This architectural choice not only enhances computational efficiency but also aligns more closely with human-like navigation, where a global plan (e.g., looking at a map) precedes local action.

E. Limitations and future work

E.1. Limitations

Though effective, our work still has the following limitations:

Reliance on a high-quality global view: The current framework fundamentally depends on the availability of a clean, top-down 2D map of the environment. This assumes such prior information is accessible, which may not be the case in many real-world applications.

Disregarding semantic information from local observations: ReasonNavi performs its MLLM-based reasoning as a one-off step before navigation begins. It does not incorporate semantic information from its egocentric view while in transit to correct or refine its global plan. For example, if the initial plan is incorrect, the agent cannot use local visual cues (e.g., seeing kitchen appliances) to recognize its mistake and re-evaluate its path. Also, it cannot use local observations to refine the reasoning process.



Figure 6. The ambiguity of the global map may influence the outcome. For example, MLLM sometimes struggles to pin-point the clothes (at the right-bottom corner) on the left map or the tv monitor (at the left-bottom corner) on the right map. (denoted with blue bounding box)

Inability to reason about objects with ambiguous top-down projections: The MLLM’s ability to locate a target is limited by the quality of the 2D map. Objects that are not clearly or have an indistinct shape from a top-down perspective can be difficult for the MLLM to identify (even though our multi-stage global reasoning consists of “zoom-in” strategy), potentially leading to inaccurate goal localization. For example, as shown in Figure 6, the recognition of the clothes or the tv sometimes is challenging for MLLMs.

E.2. Future Work

We left the following as promising future work:

Incorporating diverse global map modalities: To reduce the reliance on perfect pre-built maps, future work could explore using other forms of global information, such as architectural CAD drawings, hand-drawn sketches, etc.

Integrating global reasoning with local semantic feedback: A promising direction is to create a tighter loop between global planning and local perception. The MLLM could be invoked not just at the start but also when the agent encounters local semantic cues. This would allow the agent to re-reason and adapt its strategy mid-journey. Furthermore, this would develop interactive reasoning mechanisms where the agent can perform exploratory actions to resolve uncertainty about a potential target’s location, combining the strengths of both global foresight and local observation.